Laser Chem., Vol. 12, pp. 181–197
Reprints available directly from the Publisher
Photocopying permitted by license only

UV LASER INDUCED CHEMISTRY OF ADSORBED DIMETHYLCADMIUM

V. N. VARAKIN and A. P. SIMONOV

Karpov Institute of Physical Chemistry, Moscow, 103064, Russia

The UV laser chemistry of dimethylcadmium (DMCd) either chemisorbed at 297 K on n-type Si(100) with native oxide or physisorbed at 150 K on a photodeposited cadmium film has been studied by using mass spectrometry of desorbed species. A XeCl laser induced the heterogeneous fragmentation of these chemisorbed molecules as well as the desorption of DMCd, Cd, and CH_3. The resonant absorption of a KrCl laser radiation by adsorbed DMCd led to their photolysis and the ejection of DMCd and its fragments in both neutral and ionic forms. The kinetic, laser fluence, and time-of-flight dependences of desorbed species have been measured to elucidate the mechanisms of the dissociative and desorption processes either induced by lasers or occurring spontaneously. The effects of these lasers on chemisorbed DMCd as well as KrCl laser assisted processes in chemisorbed and physisorbed molecules have been compared.

KEY WORDS: Excimer lasers, organometallic molecules, chemisorbed and physisorbed species, adlayer photochemistry, desorption mass spectrometry.

1. INTRODUCTION

Laser-assisted chemical vapour deposition (LCVD) of thin metal films from organometallic (OM) gaseous precursors is of special interest for microelectronics since this technology makes it possible to produce films with required properties such as purity, composition, and shape.[1] The formation of the first metallic layer, based on the photochemistry of adsorbed OM, is of central importance for film properties.[2] The adlayer processes are strongly dependent on the substrate. For microelectronics, the most useful substrates are silicon, its oxide, and deposited metal films, which represent the materials of different electronic nature: semiconductor, dielectric, and metal, respectively. The study of the influence of substrate material on the dynamics of adlayer photochemistry is interesting for both applied and fundamental sciences.[3]

The mass spectrometry of the species desorbed by laser is an attractive method to probe adlayer photoprocesses. It is well concerted with the aim of the first stage of LCVD, which consists in the rupture of bonds between metal atoms and organic radicals and in the selective desorption of these radicals. Mass spectrometric investigation of the photochemistry of adsorbed OM molecules induced by UV excimer lasers have been intensively performed in the last five years.[3–9] The cross section of adlayer photolysis,[3,4] the sequences of the OM photofragmentation,[6–8] the influence of substrate material on photochemistry of adsorbates[3] have been studied. At the same time, some important aspects are let out of sight. Such problems

as an influence of surface irradiation by laser on the dynamics of adlayer processes and as a kinetics of adsorption and spontaneous fragmentation of OM species have still been practically untouched. Mechanisms of laser-induced processes are also little studied.

An approach to heterogeneous laser chemistry presented here is quite different from that of other research groups.[3–9] One principal distinguishing feature is a detailed analysis of the composition and kinetics of adlayer since this knowledge is needed to elucidate mechanisms of laser-induced processes.

It should be emphasized that the adsorption of OM molecules is often accompanied by their fragmentation. This is of special importance for the surfaces illuminated by powerful laser radiation because such a treatment leads to the formation of surface sites promoting adsorption and decomposition. Our experiments carried out earlier[10] have demonstrated that adsorption was accelerated and saturated coverage was increased with increasing of laser fluence. Moreover, as this laser irradiation ceased, the initial adsorption properties of the surface were gradually restored with a time greater than an hour, but this relaxation was not complete. The laser-induced fragmentation of adsorbed OM species may lead to the accumulation of both metal atoms and carbon-containing radicals, which influence adsorption in opposite manner. To eliminate such disappearing and accumulating effects, the substrate surface was exposed to several laser pulses of a definite fluence before every adsorption cycle. This resulted in the desorption of all the adsorbates from the surface as well as in its definite activation, so that after a fixed exposure in OM vapour, the coverage and composition of adlayer were reproduced. Therefore, of importance is the dependence of desorption yields on OM vapour exposure of the surface since it reflects the kinetics of adlayer formation and chemical reactions in it.

Another important distinguishing feature consists in the choice of the objects for investigation. Firstly, it was a monolayer of chemisorbed OM molecules being studied extremely rare[5] although the photolysis of just the same adsorbates results in the deposition of the first metal layer. Secondly, a multilayer of OM molecules physisorbed on a photodeposited metal film was under our investigation. A comparison of these chemisorbed and physisorbed species makes it possible to reveal the differences in their photochemistry as well as the role of the electronic nature of substrate in these processes.

Utilized powerful excimer lasers caused the importance of multiphoton processes. Therefore, the second main experimental dependence was that of desorption yields on laser fluence. The degree of nonlinearity of such a dependence exhibits the mechanism of a photoprocess. High-energy photons of excimer laser induced an efficient photoionization of the initial OM molecules and their fragments. As desorbed ionic fragments had been detected earlier,[8] here detailed measurements of kinetic, fluence, and time-of-flight (TOF) dependences of desorbed ions were carried out.

A general principle of our approach is the following: all the conclusions are based on the comparison between the same type dependences (kinetic, fluence or time-of-flight) measured (i) for desorbed species at different masses, (ii) for neutrals and ions, (iii) from chemisorbed and physisorbed states, (iv) at different laser excitation wavelengths, (v) for substrates of various electronic nature. The coincidence

of kinetic curves for different desorbed species demonstrates that they originate from one and the same adsorbate. The correlation of fluence dependences indicates a common desorption mechanism of the studied species. The TOF profiles allow to separate the dissociative processes occurring on the surface and in the mass spectrometer used to detect desorbed species, since in the latter case, the TOF dependences of both the initial molecules and their fragments would have at least one peak the same for all these species.

2. EXPERIMENTAL SECTION

The experiments were performed in an ion-pumped stainless steel chamber with a base pressure of 1×10^{-9} Torr. A specimen of n-type Si(100), having been optically polished using chromium oxide and washed in acetone, was mounted on a manipulator in the chamber and warmed at 150°C for 5 hours at base pressures of 10^{-7}–10^{-8} Torr. DMCd vapour was purified using freeze-pump-thaw cycles. During the experiments, the pressure of DMCd vapour in the chamber was maintained at a constant value controlled by a quadrupole mass spectrometer (QMS) (Riber QMM-17). The DMCd pressure was measured using an uncorrected ionization gauge. The radiation of an excimer laser operating on XeCl (308 nm, 60 mJ/pulse) or on KrCl (222 nm, 7 mJ/pulse) was focused onto the specimen at an angle of 45° so that laser fluence at the surface exceeded 420 and 70 mJ/cm^2, respectively. These wavelengths are strongly absorbed by silicon while the shorter one is only close to the centre of DMCd electronic absorption band.

Desorbed species were detected by the QMS positioned opposite the specimen at a distance of 3.5 cm from its surface to the center of the QMS ionizer. Pulsed desorption signals induced by the laser were measured at masses of DMCd, MMCd (the abbreviation of monomethylcadmium), Cd and CH_3 since that of C_2H_6, CH_4 and their fragments appeared to be considerably lower than CH_3 one.

The QMS was adjusted to provide the highest admittance for Cd-containing species with distinct resolution of their peaks but without isotopic structure. The fragmentation of DMCd vapour using an electron impact energy of 33 eV was characterized by the following ratios of peaks: DMCd:MMCd:Cd:CH_3 = 1:2.7:1.4:1.55. To detect desorbed ions, an emission current in the ionizer was reduced from 1 to 0.15 mA and zero potential of cathode was set. In this case, no ionization of gaseous neutrals occurred but a partial fragmentation of desorbed ions crossing the ionizer was possible.

The temporal shapes of pulsed desorption signals contain the distribution of flight times from the specimen surface to the QMS ionizer.[5–8] To determine the actual values of these times, it is necessary to take into account the duration of the drift through the quadrupole mass filter of ions formed from desorbed species in the ionizer. These drift times have been measured to be from 20 to 58 μs at masses of CH_3 and DMCd, respectively. While measuring the TOF shapes of desorbed ions, a flight distance was from the specimen up to the QMS electron multiplier. To record the TOF profiles, a preamplifier with a time constant less than 1 μs was used. In other

cases, a standard integrating preamplifier of QMM-17 was utilized. Mass spectrometric signals were recorded by a digital storage oscilloscope.

In the experiments with chemisorbed DMCd,[10,11] the Si(100) specimen was kept at 297 K and the DMCd pressure was maintained at 3×10^{-9} Torr. Before every DMCd exposure, the specimen was illuminated by 5–6 pulses at fluences of 420 mJ/cm^2 for XeCl laser and 45 mJ/cm^2 for KrCl one. This resulted in both the removal of all the adsorbates and the definite surface activation. This activation has appeared to be approximately equal for the pointed fluences of these lasers.

The experiments with physisorbed DMCd[12] were carried out on the specimen hold at 150 K and covered with a cadmium film, which had been deposited as a result of the photolysis of DMCd by KrCl laser. DMCd vapour was introduced by using a capillary positioned at 1 cm from the specimen surface. The DMCd pressure in the chamber was 1×10^{-8} Torr while not far from the specimen it was probably 1–2 orders of magnitude higher. The surface was cleaned by 3 pulses of KrCl laser at a fluence of 70 mJ/cm^2, which was not enough to remove the deposited cadmium film.

3. RESULTS AND DISCUSSION

3.1 XeCl Laser Induced Fragmentation and Desorption of Chemisorbed DMCd Molecules

The interaction of intensive XeCl laser pulses with DMCd adsorbed on silicon with native oxide resulted in some decomposition of the initial molecules as well as in the desorption of neutral species. The desorption yields have been detected at masses of DMCd, MMCd, Cd, and CH_3 and their fluence and kinetic dependences have been measured.

It should be mentioned that DMCd adsorption was accompanied by its spontaneous decomposition leading to the coexistence of the initial molecules and their MMCd, Cd, and CH_3 fragments on the surface. The behaviour of these adsorbates accounts for the experimental data.

The fluence dependences of the desorption yields are shown in Figure 1. These data are normalized to the signals measured with a fluence of 360 mJ cm^2. The ratios of these signals at the masses of MMCd, Cd, and CH_3 to that of DMCd are 2.8, 26, and 14, respectively.

The dependences of DMCd and MMCd are close to each other in the examined fluence range. Moreover, the ratio of these signals is close to that caused by DMCd fragmentation in the QMS ionizer. This indicates that both signals can be attributed to DMCd desorption followed by its decomposition in the ionizer. Therefore, either all desorbed MMCd radicals dissociate before their QMS detection or no MMCd is desorbed by the XeCl laser. To take into account the instability of vibrationally excited MMCd gaseous species,[13] the former supposition is likely to be correct. So in these experiments, the desorption of MMCd radicals caused the Cd and CH_3 signals.

The fluence ranges of the considerable Cd and CH_3 desorption growth are quite

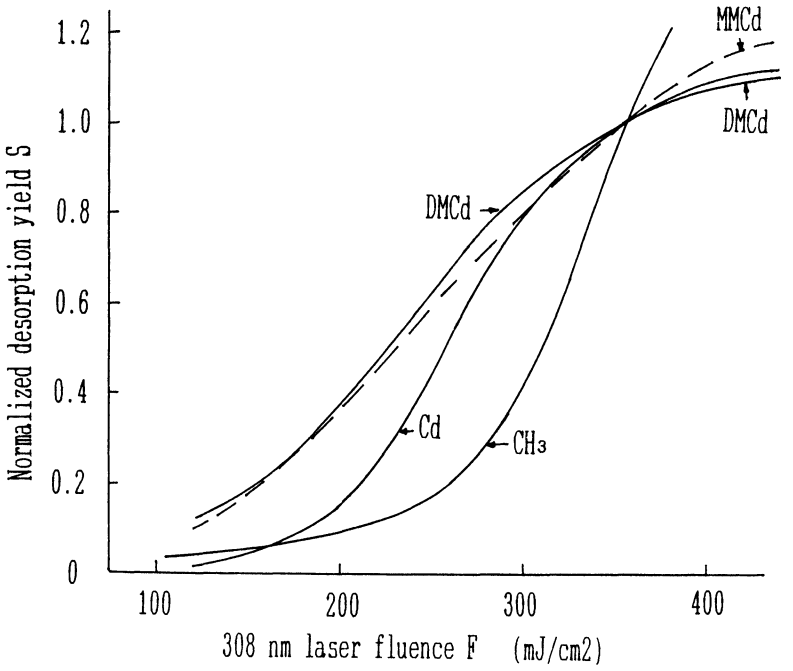

Figure 1 XeCl laser fluence dependences for chemisorbed species measured at a DMCd exposure of 0.1 L (1 L = 10^{-6} Torr·s).

different demonstrating that individual desorption pathways of these species predominate at fluences F = 200–300 mJ/cm^2. As DMCd and MMCd are likely to bind to the surface through Cd atom, it is hard to imagine any mechanism preferring the Cd fragment desorption from these adsorbates. Therefore, the sources for these individual pathways should be the adsorbed Cd and CH_3 species which are formed from DMCd spontaneously or due to laser irradiation. The latter case predominates at short exposure times and high laser fluences. This desorption should occur stepwise. At first, the laser-induced fragmentation up to Cd and CH_3 adsorbates should perform, then these species should be independently desorbed by the same laser pulse. The higher energy needed for CH_3 desorption than for Cd one suggests that CH_3 radicals are more tightly bound to the surface.

At as low fluences as 120 mJ/cm^2, when the desorption of CH_3 adsorbates is quite inefficient, the ratios of Cd and CH_3 to DMCd yields already exceeds by 2.5 times the values caused by DMCd fragmentation in the QMS. This proposes that the desorption of vibrationally excited DMCd or MMCd followed by their fragmentation in gaseous phase is important. The further increase of these ratios by an order of magnitude with increasing fluence can be attributed to the individual Cd and CH_3 desorption pathways.

The ratios of CH_3 to both DMCd and Cd signals have minima at 200 and 260 mJ/cm^2, respectively, proposing the existence of CH_3 desorption pathway at

$F < 120$ mJ cm^2 as well as of more efficient mechanisms of Cd and DMCd desorption at higher fluences. To justify these proposals, the release of CH_3 from adsorbed DMCd or MMCd should precede the desorption of intact DMCd molecules and Cd atoms. We believe that this CH_3 release is based on the photoexcitation of DMCd molecules due to absorption in the wings of their electronic band[14] rather than of silicon substrate. Another possibility deals with the desorption of excited DMCd or MMCd leading to both CH_3 and Cd signals and with the recombination desorption of DMCd and the desorption of Cd adsorbates, which may provide more rapid increases of Cd and DMCd signals than CH_3 one at higher fluences.

The fluence dependences of DMCd and Cd are characterized by the degrees of nonlinearity of 2 and 4.5 ± 0.5, respectively, which remain constant up to $F = 280$ mJ/cm^2, and then they exhibit saturation. The dependence of CH_3 is described by two different degrees: NL = 1.5 at $F < 220$ mJ/cm^2 and NL = 4.5 at $F > 220$ mJ/cm^2, which reflect the existence of two different mechanisms of CH_3 desorption. The dependence close to linear at low fluences argues in favour of the photolytic mechanism of the CH_3 release from adsorbed DMCd molecules.

The kinetic dependences obtained with a laser fluence of 420 mJ/cm^2 are shown in Figure 2. The curves of DMCd and MMCd coincide further confirming their

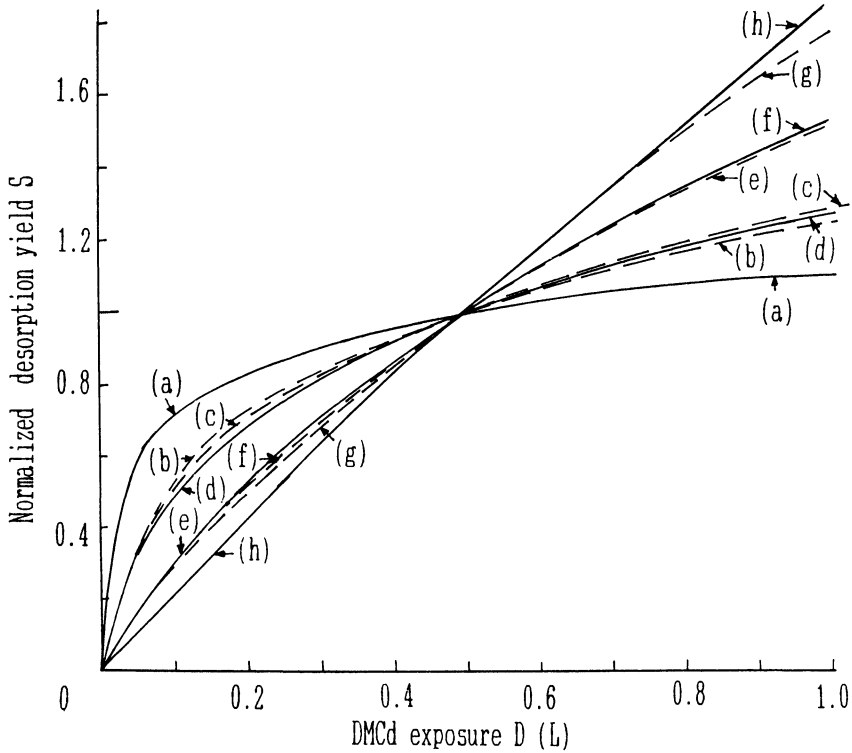

Figure 2 Kinetic dependences of desorption yields induced by XeCl (dashed lines) and KrCl (solid lines) lasers: (a) Cd^+, (b) MMCd, (c) DMCd, (d) CH_3, (e) $MMCd^+$, (f) CH_3, (g) Cd, (h) CH_3^+.

common desorption mechanism. DMCd adsorbates as the most rapidly formed adspecies is likely to be the source for DMCd desorption. Therefore, the intact desorption rather than the recombination one is a leading pathway of DMCd desorption.

The simultaneous growth of Cd and CH_3 signals for gaseous doses up to D = 0.5 L may be explained in two ways. Firstly, these species may be produced from one and the same adsorbate. DMCd having the adsorption kinetics quite different from that of Cd and CH_3 cannot be such an adsorbate. So the only MMCd containing Cd and CH_3 as its constituents can. Then the stepwise desorption of MMCd adsorbates or their dissociative desorption would provide the coincidence of Cd and CH_3 kinetics. Secondly, as all the fragments remain on the surface, the individual Cd and CH_3 desorption pathways would also synchronize these kinetic curves. Their discord at D > 0.5 L may be rationalized in terms of the spontaneous decomposition of chemisorbed molecules accompanied by the recombination desorption of CH_3 radicals whereas Cd fragments stick well to the earlier deposited ones. The existence of different kinetic curves reveals the spontaneous fragmentation of DMCd adsorbates up to Cd and CH_3 ones. At short exposure times, when all the signals are related to DMCd adsorbates, the ratios of Cd and CH_3 to DMCd yields considerably exceed that obtained due to the fragmentation in the QMS. Hence, the stepwise or dissociative processes are extremely efficient. The further increase of these ratios is caused by the desorption of MMCd, Cd, and CH_3 adsorbates successively appearing in the course of the spontaneous decomposition of the initial molecules.

3.2 Resonance-Enhanced Interaction of KrCl Laser with Chemisorbed DMCd Molecules

The absorption of KrCl laser radiation by adsorbed DMCd resulted in their extreme fragmentation followed by the desorption of Cd and CH_3 fragments only. The fluences of KrCl laser inducing the dissociation and desorption were an order of magnitude lower than that of XeCl laser. Another special feature of 222 nm photoreactions in adlayer consisted in the desorption of $MMCd^+$, Cd^+, and CH_3^+ ions.

The kinetic dependences of the desorption yields of neutral and charged species obtained at the KrCl laser fluence of 36 mJ/cm^2 are brought together with the data received with XeCl laser in Figure 2. At the saturated adsorbate coverages, the ratios of the desorption signals of CH_3, $MMCd^+$, and CH_3^+ to that of Cd^+ are 0.033, 0.009, and 0.055, respectively.

The dependences of some species are close to one another indicating the existence of the common adsorbates as sources of their desorption. The curve of DMCd (308 nm laser excitation) coincides with CH_3 one (222 nm) demonstrating that the KrCl laser induced release of CH_3 radicals occurs from chemisorbed DMCd molecules. The similarity of the kinetic curves of Cd, CH_3 (308 nm) and $MMCd^+$ (222 nm) at D < 0.5 L suggests MMCd adsorbate to be the main source of these signals. At higher exposures, the Cd signal increases more rapidly than two others, which continue to be close to each other. This demonstrates that CH_3 adsorbates having been formed spontaneously leave the surface while Cd fragments accumulate on the

surface providing an additional laser-induced desorption yield. This difference in the behaviour of Cd and CH_3 adsorbates can be attributed to the adsorption geometry of MMCd radical through the cadmium atom and it exhibits itself because of lack of unoccupied adsorption sites at high coverages.

An adsorbate which causes the generation of Cd^+ ions is evidently formed more rapidly than DMCd chemisorbs. There are some reasons that both DMCd molecules in weakly bound state, which preceeds strong chemisorption, and Cd atoms themselves might be appropriate adsorbates. Cd atoms may accumulate on the surface due to either their deposition from gaseous phase, where they are produced as a result of DMCd photolysis by KrCl laser pulses used for the sample cleaning, or their diffusion from unirradiated surface regions. However, molecules in weakly bound states cannot form high adsorbate coverages as well as the low DMCd vapour pressure and large dimensions of the irradiated area prevent fast formation of high Cd coverages. Therefore, the high Cd^+ signals can only be rationalized by the resonance enhancement of the photoprocesses.

A mechanism of the photogeneration of Cd^+ ions in DMCd vapour by KrCl laser has been proposed previously.[15] It consists of three absorption steps. The first laser photon excites DMCd molecules into $B^1\pi_u$ state extremely fast dissociating into MMCd in A^2E state and CH_3 radical. The second one induces the further fragmentation of MMCd to Cd in the excited state $^3P_1$ and CH_3. At least, the one-photon ionization of these electronically excited Cd atom occurs. This mechanism provides the high efficiency of Cd^+ photogeneration due to vibronic resonances in both DMCd and MMCd. Such resonances are absent in atomic Cd. Therefore, the DMCd precursors are likely to be the adsorbates leading to the desorption of Cd^+ ions.

It is reasonable to attribute the most slow process characterized by CH_3^+ desorption signal to the poor accumulation of chemisorbed CH_3 as a result of spontaneous DMCd fragmentation. It should be mentioned that the measured kinetic curve of Cd neutrals is highly distorted by the intensive Cd^+ signal, which has not been completely suppressed in the QMS at the chosen voltages of the ionizer.

In summary, the kinetics of the DMCd adsorption and spontaneous fragmentation on silicon with native oxide is characterized by the following order: (i) the adsorption of DMCd in the precursor state probed by photogeneration of Cd^+, (ii) the chemisorption of DMCd reflected by the desorption signals of DMCd/MMCd (308 nm) and CH_3 (222 nm), (iii) the DMCd spontaneous decomposition to MMCd adsorbates probed by $MMCd^+$ desorption (222 nm), (iv) the formation of adsorbed Cd fragments described by the difference between kinetic curves of Cd (308 nm) and $MMCd^+$ (222 nm), (v) at least, the slow accumulation of CH_3 adsorbates (since a great number of them desorbs by the recombination pathway) probed by CH_3^+ signal (222 nm).

The fluence dependences of KrCl laser induced desorption obtained at saturated adsorbate coverages are depicted in Figure 3. The only linear dependence describes the one-photon release of CH_3 radicals due to resonant photoexcitation of chemisorbed DMCd. All other desorption processes have some fluence thresholds, which are determined by both the nonlinearity of photoprocess and the QMS

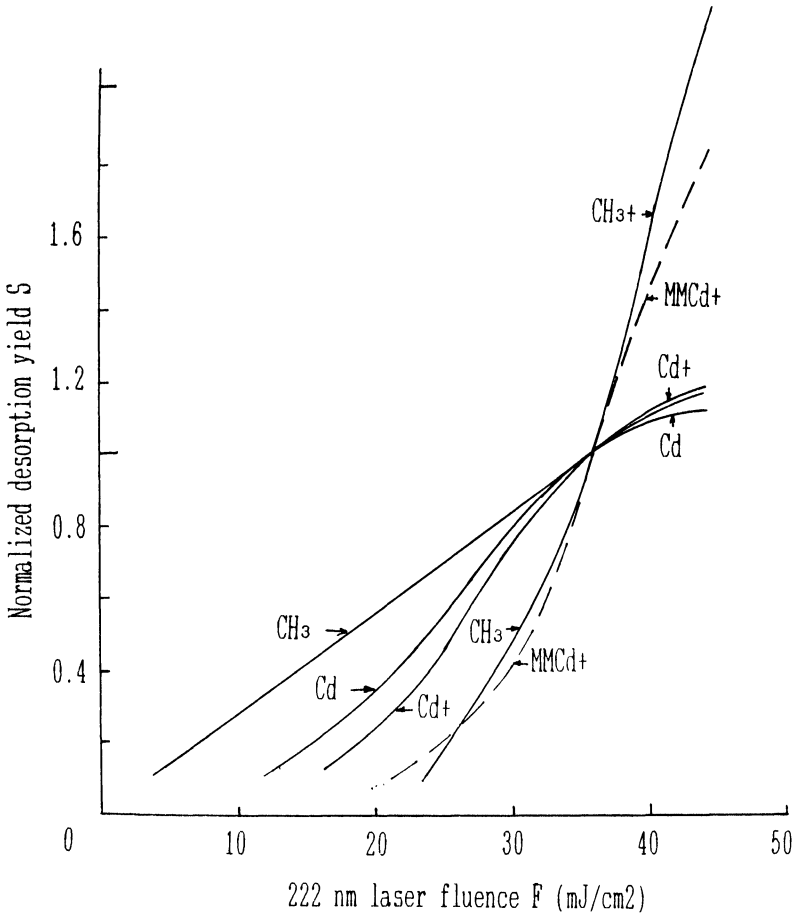

Figure 3 KrCl laser fluence dependences obtained for chemisorbed species at saturated coverages.

detection limit. At low fluences, a cubic dependence has been observed for the desorption of Cd^+ ions and a square one for Cd neutrals that are in agreement with the discussed three-photon mechanism of Cd^+ generation through the two-photon production of Cd ($^3P_1$) as the intermediate. The high values NL = 4.5 ± 0.5 for $MMCd^+$ and CH_3^+ signals may be attributed to their desorption induced by the laser excitation of silicon and the lack of resonances in chemisorbed MMCd. The distinction of resonant properties of adsorbed DMCd and MMCd under KrCl laser irradiation obviously exhibits itself in both the hundredfold superiority of Cd^+ signal over $MMCd^+$ one and the saturation of the Cd^+ yield at F = 30 mJ/cm^2 while $MMCd^+$ signal continues to increase. The correlation of the fluence dependences of $MMCd^+$ and CH_3^+ in the middle of the studied range may indicate that CH_3^+ ions appears as a result of the decomposition of vibrationally excited $MMCd^+$ ones. Then some discord at lower fluences may be accounted for the insufficiently high vibrational excitation of $MMCd^+$. At higher laser fluences, it is likely that the

desorption of chemisorbed CH_3 radicals followed by their photoionization prevails over their production from MMCd adsorbates.

3.3 308 versus 222 nm Laser Excitation

The main distinctions between KrCl and XeCl lasers in their interaction with chemisorbed DMCd are the following: (i) much lower fluences of KrCl laser compared with XeCl one are needed to dissociate DMCd molecules and to desorb adsorbates, (ii) KrCl laser completely decomposes all the initial molecules since no intact DMCd species have been desorbed, (iii) ion desorption is induced by KrCl laser only. These distinctions can be explained by the resonant DMCd excitation using KrCl laser and by the difference in the energies of KrCl and XeCl laser photons, which are equal to 5.6 and 4.0 eV, respectively. The latter makes it possible the two-photon ionization of the studied species at 222 nm only. KrCl laser resonantly interacts with DMCd in both precursor and chemisorbed states rather than with chemisorbed MMCd. This induces the efficient desorption of Cd in ionic and neutral forms as well as of CH_3 radicals. The lack of CH_3 signal from DMCd precursors can be explained by their low coverages whereas Cd^+ signal has been observed due to the 2–3 order higher sensitivity of the QMS for ion detection compared with neutrals. The absence of Cd^+ signal originated from chemisorbed DMCd may be attributed to quenching of photoreaction intermediates in chemisorbed adlayer. Weak absorption of XeCl laser radiation in the wings of the absorption bands of chemisorbed DMCd and MMCd molecules may to some extent cause the decomposition of these adsorbates and release of CH_3 at low fluences. However, the basic desorption mechanism at 308 nm seems to be connected with silicon photoexcitation. The analogous one is expected to play the critical role in the desorption of $MMCd^+$ and CH_3^+ at 222 nm. As XeCl laser pulse with $F = 400\ mJ/cm^2$ is able to heat the silicon surface up to its melting point and to induce the thermal desorption of adsorbates, the temperature rise obtained with KrCl laser at $F = 45\ mJ\ cm^2$ is too small for the thermal desorption. We believe that the basic desorption mechanism at both wavelengths is based on the photogeneration of electron-hole pairs in silicon and their interaction with adsorbates.

As to the generation of ions, it should be noted that, although 222 nm is close to both the centres of DMCd and CH_3 absorption bands and the sum energy of two photons is above the ionization potentials of these species, their resonance-enhanced two-photon ionization have not been observed due to both the competition of the dissociative process leading to the lifetimes of the resonant vibronic levels as small as 100 fs[16,17] and the small values of the Franck-Condon factors for the absorption of the second photon.

3.4 Laser Chemistry of DMCd Physisorbed at 150 K on Cadmium Film

Laser-induced processes in a multilayer exhibited some new features such as desorption of intact DMCd and MMCd neutrals as well as $DMCd^+$ ions. The nonmonotonous behaviour of some kinetic and fluence dependences has also been

discovered. The TOF profiles of desorbed neutral and ionic species have been measured.

The fluence dependences of desorption yields are depicted in Figure 4. The ratios of the maximum values of these yields are the following: $Cd^+ : DMCd^+ : MMCd^+ : CH_3^+ : DMCd : MMCd : CH_3 = 1:0.05:0.45:0.45:0.07:0.27:0.5$.

The CH_3 signal is proportional to laser fluence at $F < 15\ mJ/cm^2$, in the range $F = 20–50\ mJ/cm^2$, it varies quadratically and further it exhibits saturation. The ejection of the first and second CH_3 radicals by the stepwise photoexcitation of DMCd can be responsible for the observed dependence. The desorption yields at DMCd and MMCd masses both appear at $F > 10\ mJ/cm^2$ and increase similarly up to $F = 25\ mJ/cm^2$ but the saturation of DMCd signal occurs earlier than that of MMCd. This indicates that the common desorption pathway is changed at $F > 25\ mJ/cm^2$ by individual ones.

The fluence dependences of $DMCd^+$ and $MMCd^+$ exhibit an unusual behaviour. They are characterized by the signal local maxima at $F = 20\ mJ/cm^2$, by their almost

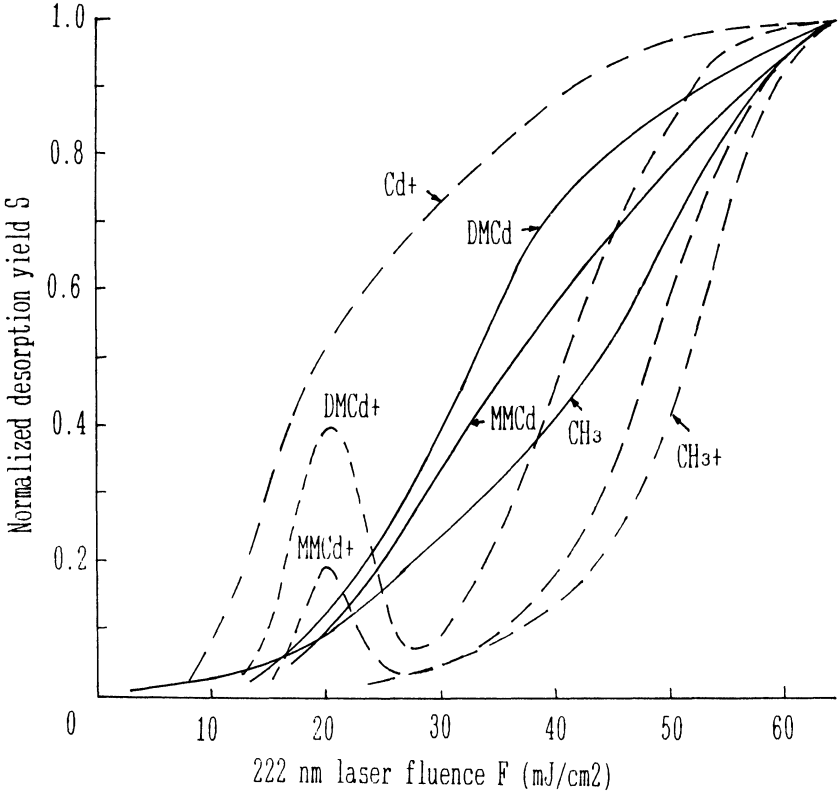

Figure 4 KrCl laser fluence dependences of ionic (dashed lines) and neutral (solid lines) desorption yields measured for physisorbed species at a DMCd exposure time of 15 s.

full disappearance at $F = 30\ mJ/cm^2$, and by further intensive increase. Again, the similar behaviour of these curves at $F < 30\ mJ/cm^2$ demonstrates their common origin from desorbed $DMCd^+$ species whereas the different mechanisms of $DMCd^+$ and $MMCd^+$ desorption are responsible for the discord of these curves at higher fluences.

At low $F < 20\ mJ/cm^2$, the Cd^+ yield grows like $DMCd^+$ and $MMCd^+$ ones but further it only slightly slows down its increase whereas the compared signals essentially decrease. The absence of the similar minimum for the fluence curve of Cd^+ was found to be due to fast Cd^+ yield growth induced by an individual desorption pathway predominating at $F > 30\ mJ\ cm^2$. The saturation of Cd^+ signal occurs at the lower laser fluence compared with other ions emphasizing the resonance enhancement of the individual mechanism of Cd^+ photogeneration. Quite on the contrary, the saturation of CH_3^+ yield is observed at the highest fluences. The dependence of CH_3^+ desorption is characterized by two degrees of nonlinearity equal to 3.3 and $5.5 + 0.5$ for fluences lower and higher than $45\ mJ/cm^2$. The three-photon mechanism of CH_3^+ generation may be similar to that proposed previously for KrF laser induced photogeneration of Cd^+ and CH_3^+ ions in DMCd vapour,[15] provided that such an intermediate as excited MMCd species would rapidly decay into the ground electronic state due to collision-induced relaxation in the multilayer. Then the absorption of two photons by MMCd radicals would result in the generation of the vibrationally excited $MMCd^+$ ions instantly dissociating into two pairs: CH_3^+ and Cd as well as CH_3 and Cd^+. The high values of the nonlinearity degrees $NL > 5$ describing the desorption of $DMCd^+$, $MMCd^+$, and CH_3^+ ions are hard to relate to the appropriate multiphoton processes since their efficiencies at the used laser intensities are too small to be detected. The laser excitation of substrate is likely to be important.

The kinetic dependences measured at the saturating fluences are shown in Figure 5. Moreover, the dependence of $MMCd^+$ yield has also been obtained at $F = 20\ mJ/cm^2$ corresponding to the local maximum in the fluence dependence. It should be emphasized that all the signals except that for Cd^+ are absent at zero exposure indicating the desorption of all the adsorbates by the laser pulses used for the surface cleaning while the deposited cadmium film remains. By subtracting the background Cd^+ signal from the kinetic curve of Cd^+ and renormalizing, one can receive the curve which coincides with that of CH_3^+. This indicates that Cd^+ and CH_3^+ originate from one and the same adsorbate. As this adsorbate kinetics is the most rapid, DMCd in the precursor state is likely to be such an adsorbate. The similar kinetic curves of DMCd and MMCd demonstrate that both these species originate from adsorbed DMCd. Hence, the individual pathway of MMCd desorption at high fluences includes the laser-assisted dissociation of DMCd adsorbates. The kinetic dependence of CH_3 at short exposure times $t < 10$ s is close to that of DMCd one indicating that the CH_3 radicals generated by two-photon mechanism also originate from DMCd adsorbate. The slower growth of CH_3 signal compared with DMCd one at longer times may be attributed to the low efficiency of CH_3 generation in the internal adlayers due to quenching dissociation by collisions.

The dependences of $DMCd^+$ and $MMCd^+$ are distinguished from the others by their initial delay in the signal growth. This can be explained by their generation in any adlayer except the neighbouring to cadmium film since the second adlayer begins to

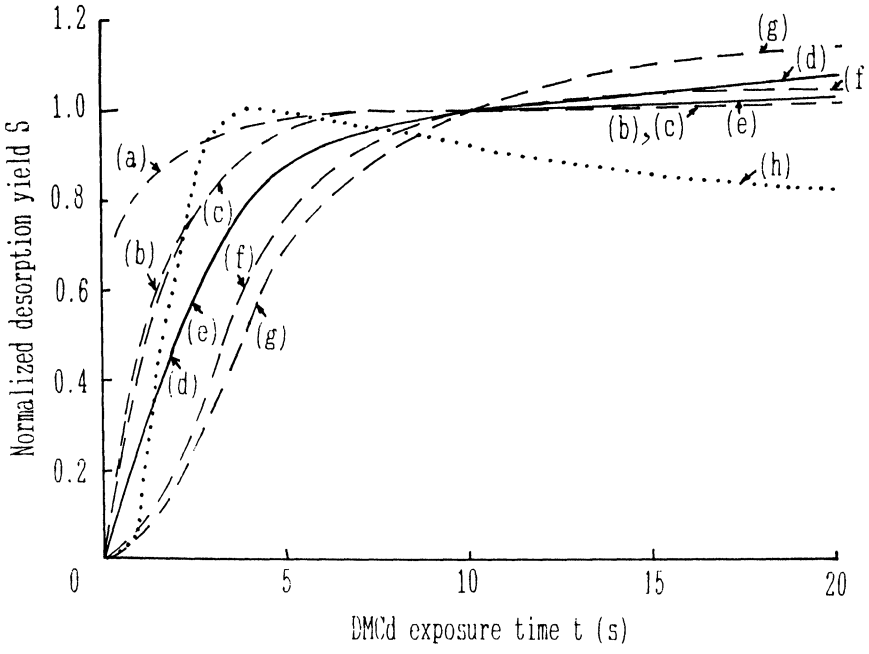

Figure 5 Kinetic dependences of ionic (dashed lines) and neutral (solid lines) desorption yields obtained for physisorbed species at a KrCl laser fluence of 65 mJ cm^2: (a) Cd^+, (b) Cd^+ (without background), (c) CH_3^+, (d) DMCd/MMCd, (e) CH_3, (f) $DMCd^+$, (g) $MMCd^+$. The dotted line (h) represents the kinetic curve of $MMCd^+$ desorption yield measured at F = 20 mJ/cm^2.

form after the first one has partially been fulfilled. The most interesting kinetic curve is that of $MMCd^+$ measured at F = 20 mJ/cm^2. This $MMCd^+$ signal, being slightly delayed at first, rapidly increases to its maximum value at t = 4 s and then slowly and monotonously decreases. The most striking fact is this decrease of the desorption signal while the appropriate adsorbate coverage continues to grow. This may be attributed to the scattering of the desorbing ions under collisions with other species since their desorption flux considerably grows with increasing coverages at t = 2–6 s. Similarly, one may explain the maxima in the fluence dependences of Cd-containing ions. Another possible reason may be based on the mechanism of these ions formation involving species photoejected from the substrate.[18] Then the scattering in course of the diffusion of species would restrict the penetration depth of the species ejected from the substrate as well as the ejection of the studied ions into gaseous phase. The maximum in the appropriate fluence dependences may then be attributed to the radiation-stimulated decrease of the population of adsorbed molecules in some specific state, if the interaction of such molecules with species ejected from the substrate results in the generation of the studied ions.

To provide an additional insight into the mechanisms of laser-induced processes, it is useful to study the TOF distributions of desorbed neutrals and ions. The TOF profiles have been measured at high coverages and at several values of KrCl laser fluence.

The TOF profiles of DMCd and MMCd are satisfactory described by Maxwell-Boltzmann distributions. At $F < 25\ mJ/cm^2$, their arrival times t_m corresponding to the maxima of the TOF profiles appear to be equal. This further confirms the common mechanism of their desorption. At $F > 25\ mJ/cm^2$, the values $t_m \cdot m^{-1/2}$ for those molecules are close, here m is the mass of desorbed species. As these values determine Maxwell-Boltzmann temperatures, then these molecules should be able to level up their translational energies before they leave the surface. The maximum temperature derived from these arrival times is equal to 800 K. An estimate of silicon surface temperature jump induced by the KrCl laser gives the value of 500 K. The absorption of laser radiation by the cadmium film, which is separated from silicon by the film of silicon oxide with relatively low thermal conductivity, would cause the higher peak surface temperature and its more slow cooling. Hence, the thermal desorption of physisorbed molecules under KrCl laser irradiation may occur but the fragmentation of adsorbed DMCd is photolytic rather thermal process.

The TOF profiles of CH_3 do not intersect with that of DMCd and MMCd indicating that the majority of CH_3 radicals are formed on the surface rather than in the QMS. At $F < 20\ mJ/cm^2$, the TOF profiles of CH_3 shown at Figure 6a were found to be wider compared with the Maxwell-Boltzmann ones with the appropriate arrival times due to both fast and slow desorbed CH_3 species. Such a distribution for CH_3 radicals, generated by the one-photon mechanism, may be attributed to the scattering of the radicals while diffusing to the top adlayer. At $F > 20\ mJ/cm^2$, a fine structure of these TOF profiles appears. It consists of three main peaks with widths much narrower than that would predicted by Maxwell-Boltzmann statistics. The peak positions are slightly changed with increasing laser fluence. The multimodal structure of TOF profiles are caused by the appropriate distribution of desorbed species in both the velocities and directions of their flight off. Peaks at arrival times 60 and 40 μs alter in similar manner. Just these two peaks are described by the fluence and kinetic dependences shown in Figures 4 and 5. The narrow widths of these peaks further confirm the photolytic mechanism of radical formation as well as their generation in the top adlayers. The latter statement may be explained in terms of the collision-induced desactivation of the long-lived state A^2E of MMCd serving as an intermediate in the two-photon generation of CH_3. The intensity of a 28 μs peak has a maximum at $F = 40\ mJ/cm^2$, however, the reason of such a behaviour is not clear since the desorption mechanism of such CH_3 is not known. The superposition of various peaks prevents the measurement of the kinetic and fluence dependences of species which are not described by the most intensive TOF peaks. The intensive Cd^+ signal screens a maximum in the TOF profiles of Cd neutrals making impossible to study them.

The TOF profiles of ions desorbed by a laser have an essential peculiarity since the initial distribution of ion velocities is influenced by an acceleration of these ions in a local charge field.[8] This electric field is created because photoemitted electrons quit the surface fast enough to leave a large positive charge. It disappears very fast after laser pulse due to excessive charge dispersion. As a result of the transient behaviour of this field, the difference in the desorption moments for ions at the

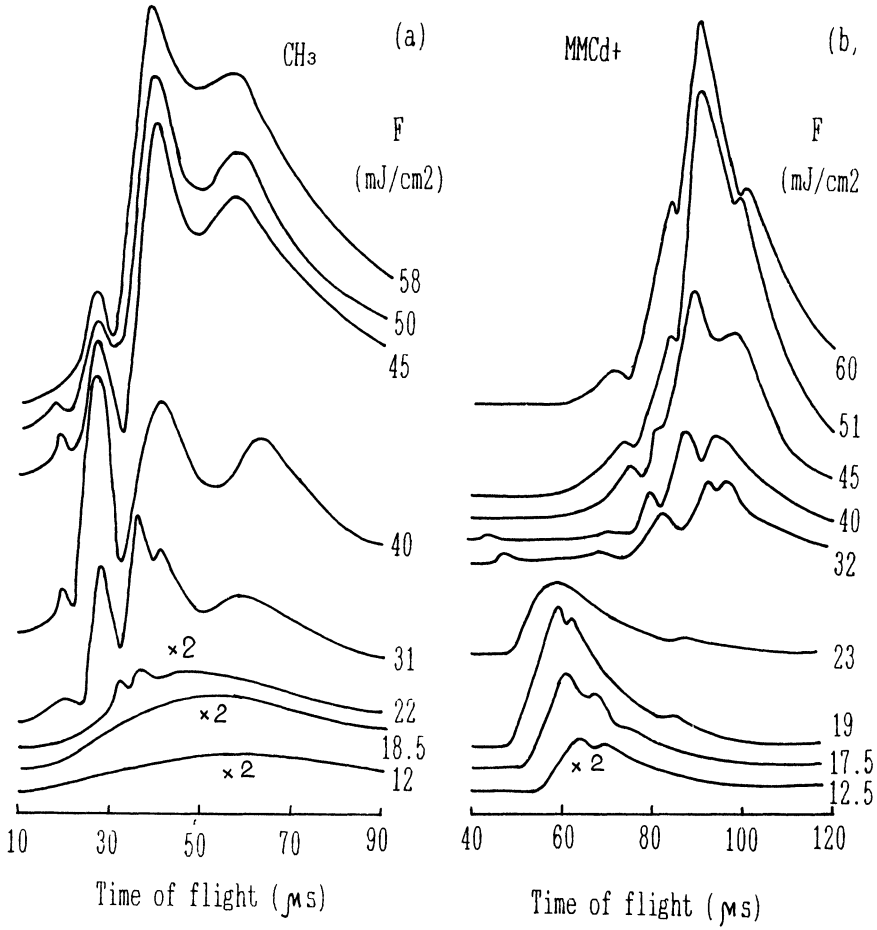

Figure 6 TOF profiles of CH_3 (a) and $MMCd^+$ (b) species measured at a DMCd exposure time of 15 s.

nanosecond time scale serves an additional reason of fine TOF structure since the translational energy of ion is determined by a surface potential in the moment of ion desorption.

The TOF profiles of cadmium-containing ions manifest two main peaks as shown in Figure 6b for $MMCd^+$. Their first peaks dominating at $F < 25$ mJ/cm^2 are formed by ions with arrival times tm = 60 μs being the same for $DMCd^+$, $MMCd^+$, and Cd^+ species. This indicates that the desorption of $DMCd^+$ ions followed by their fragmentation in the QMS induces all these signals. The second peaks describe TOF profiles at $F > 30$ mJ/cm^2. The shapes of these peaks as well as their arrival times in the range 80–95 μs are different demonstrating individual desorption mechanisms of these ions. The TOF profiles of CH_3^+ consist of two peaks with arrival times 20 and 23 μs slightly and simultaneously decreasing with increasing laser fluence. At $F = 25$ mJ/cm^2, a maximum of the ratio of these peaks intensities is observed, while

at $F > 45\ mJ/cm^2$, an accelerated growth of the second peak occurs indicating that just it determines the high degree of nonlinearity of the fluence dependence. Hence, the different desorption pathways of neutral and ionic species have the appropriate distinct peaks in the TOF profiles.

3.5 222 nm Photochemistry of Chemisorbed versus Physisorbed Molecules

Two principal reasons responsible for the differences between chemisorbed and physisorbed species are likely to be the strength of adsorption bonds and the frequency of adsorbate collisions. In a chemisorbed monolayer of DMCd at room temperature, DMCd and its fragments are tightly bound to silicon with native oxide, especially to oxygen and silicon atoms with dangling bonds, whereas the interaction adsorbed species in a loosely-packed monolayer is weak enough. In a physisorbed multilayer at 150 K, quite on the contrary, the adsorbate bonds to deposited cadmium atom as well as between the layers are weak whereas the probability of adsorbate collisions, including that in course of their diffusion from the inner layers to the top one in the desorption process, is higher. Moreover, the special features of the extreme layers should be emphasized: in the one closest to the cadmium film electronic quenching may be efficient due to the closeness of the electronic absorption of DMCd and Cd, while in the top layer, the role of collision is highly weakened. The strength of adsorption is clearly revealed in thermal desorption and collision-induced relaxation can critically change the course of photolytic processes.

The special features of photoprocesses in a physisorbed multilayer compared with those in a chemisorbed monolayer are the following: (i) the desorption of DMCd and MMCd neutrals and $DMCd^+$ ions, (ii) the increase of CH_3, $MMCd^+$, and CH_3^+ desorption yields relative to Cd^+ one by an order of magnitude, (iii) the two-photon and three-photon mechanisms of CH_3 and CH_3^+ desorption, respectively, (iv) the nonmonotonous laser fluence and kinetic dependence for Cd-containing ions and CH_3, (v) the time delay in $DMCd^+$ and $MMCd^+$ signals growth.

4. CONCLUSIONS

The main results of the investigation of laser-induced processes in chemisorbed and physisorbed DMCd molecules are: (1) the chemisorption of DMCd on UV laser preirradiated silicon with native oxide is accompanied by its spontaneous decomposition up to Cd and CH_3 adsorbates, the kinetics of these dissociative processes can be probed by the laser-induced desorption of various species, (2) XeCl laser induced DMCd fragmentation leads to both the accumulation of chemisoorbed fragments and desorption of Cd and CH_3, (3) greater XeCl laser fluences are needed for the desorption of CH_3 adsorbates than that of Cd ones, (4) MMCd desorption induced by XeCl laser is accompanied by their complete fragmentation to Cd and CH_3, (5) KrCl laser resonantly excites DMCd in precursor and chemisorbed states inducing their extreme fragmentation and the desorption of CH_3, Cd, and Cd^+ by photolytic mechanisms, (6) the selective release of CH_3 from the chemisorbed DMCd

rather than from MMCd proceeds at low KrCl laser fluences due to its one-photon mechanism in contrast with the other desorption processes, (7) KrCl laser induces the photoionization of desorbed species including the desorption of $DMCd^+$ from a physisorbed multilayer only, (8) the KrCl laser assisted desorption of $DMCd^+$ and MMCd from physisorbed rather than chemisorbed adlayers is probably connected with both collisional relaxation of molecular excited states and weak adsorption bonds, (9) the photochemistry of physisorbed molecules strongly depends on their position in the multilayer, which exhibits in such special features of Cd-containing ion desorption as the initial delay of its growth and nonmonotonous dependences of the desorption yields on DMCd exposure of the surface, (10) each adlayer process leads to its own TOF peak with characteristics elucidating its mechanism.

References

1. D. J. Ehrlich, R. M. Osgood and T. F. Deutsch. *J. Vac. Sci. Technol.*, **21**, 23 (1981).
2. D. J. Ehrlich, R. M. Osgood and T. F. Deutsch. *Appl. Phys. Lett.*, **38**, 964 (1981).
3. F. C. Celii, P. M. Whitemore and K. C. Janda. *J. Phys. Chem.*, **92**, 1604 (1988).
4. J. R. Creigton. *J. Appl. Phys.*, **59**, 410 (1986).
5. G. S. Higashi. *J. Chem. Phys.*, **88**, 422 (1988).
6. T. E. Orlowski and D. A. Mantell. *J. Vac. Sci. Technol.*, **7A**, 2598 (1989).
7. Y. Zhang and M. Stuke. *J. Phys. Chem.*, **93**, 4503 (1989).
8. J. S. Horwitz, E. Villa and D. S. Y. Hsu. *J. Phys. Chem.*, **94**, 7214 (1990).
9. J. R. Swanson, F. A. Fligtsch and C. M. Friend. *Surf. Sci.*, **226**, 147 (1990).
10. A. P. Simonov and V. N. Varakin. *SPIE Proc.*, **1352**, 274 (1990).
11. V. N. Varakin and A. P. Simonov. *Zhurn. Fiz. Khim.*, **65**, 1137 (1991) (in Russian).
12. V. N. Varakin and A. P. Simonov. To be published.
13. R. L. Jackson. *J. Chem. Phys.*, **92**, 807 (1990).
14. Y. Rytz-Froidevaux, R. P. Salathe, H. H. Gilgen and H. P. Weber. *Appl. Phys. Lett.*, **27A**, 133 (1982).
15. G. A. Abakumov, V. A. Lunchev, B. I. Polyakov and A. P. Simonov. *Opt. i Spektr.*, **65**, 578 (1990) (in Russian).
16. A. Amirav, A. Penner and R. Bersohn. *J. Chem. Phys.*, **90**, 5232 (1989).
17. J. Danon, H. Zacharias, H. Rottke and K. N. Welge. *J. Chem. Phys.*, **76**, 2399 (1982).
18. E. P. Marsh, T. L. Gilton, M. R. Schneider and J. P. Cowin. *Phys. Rev. Lett.*, **61**, 2725 (1988).